Structure and dynamics of ice Ih films upon HCl adsorption between 190 and 270 K. I. Neutron diffraction and quasielastic neutron scattering experiments

Benjamin Demirdjian, Daniel Ferry, Jean Suzanne, Céline Toubin, Sylvain Picaud, Paul N. M. Hoang, Claude Girardet

Structure and dynamics of ice Ih films upon HCl adsorption between 190 and 270 K. I. Neutron diffraction and quasielastic neutron scattering experiments

B. Demirdjian, D. Ferry, and J. Suzanne
CRMC2-CNRS,[a] *Campus de Luminy, Case 913, F-13288 Marseille Cedex 9, France*

C. Toubin, S. Picaud, P. N. M. Hoang, and C. Girardet[b]
Laboratoire de Physique Moléculaire—UMR CNRS 6624, Faculté des Sciences, La Bouloie, Université de Franche-Comté, F-25030 Besançon Cedex, France

(Received 27 June 2001; accepted 7 January 2002)

Neutron diffraction and quasielastic neutron experiments are performed to investigate the effect of HCl adsorption on the structure and dynamics of an ultra-thin ice Ih film (5 H_2O bilayers thick) deposited on a crystalline MgO(001) substrate. Three HCl coverages have been studied 0.3, 0.6, and 1 monolayer (ML) in the temperature range 190–270 K. At 0.3 and 0.6 HCl monolayer, no mobility is measured at $T \leqslant 220$ K. A translational mobility, which is a signature of a liquid phase, is observed at $T = 250$ K. This phase occurs 15 K below the surface melting temperature of the bare ice film. The fraction of mobile molecules represents 30% (0.3 ML HCl) and 45% (0.6 ML HCl) of the film. At 1 HCl monolayer and $T = 220$ K, HCl–dihydrate coexists with ice Ih, whereas at $T = 250$ K the ice film becomes amorphous and only 9% of the film is mobile. The results are discussed within the context of atmospheric chemistry. © *2002 American Institute of Physics.*
[DOI: 10.1063/1.1454990]

I. INTRODUCTION

The interaction of HCl with crystalline water ice has attracted much attention since the mid 1980s owing to its importance in heterogeneous reactions occurring on the surface of polar stratospheric clouds (PSC) and controlling the amount of ozone in the stratosphere.[1–3] PSCs are supposed to be composed of nitric acid/ice mixture (PSC I), likely nitric acid trihydrate (NAT) or pure ice (PSC II).[4–6] It is believed now that the surface of ice plays a crucial role in the ozone chemistry involved in the annual depletion of both Antarctic and Arctic ozone[6–9] and experiments have suggested that HCl uptake on ice is limited to about the equivalent of one monolayer surface coverage probably because of the weak solubility of HCl in bulk ice.[8]

Most of the experiments on the adsorption of HCl on ice were done at much lower temperatures than those currently considered in the stratosphere. Using infrared spectroscopy, Devlin and co-workers[10] identified the conditions under which molecular complexation (HCl/H_2O) competes with acid ionization. Below 50 K, the experimental results indicated the stabilization of the molecular complex HCl H-bonded to the ice surface oxygen sites, while above 60 K, HCl ionized and formed amorphous hydrate surface layers of a 1 : 1 composition. Graham and Roberts[11–13] used temperature programmed desorption and single reflection Fourier transform infrared spectroscopy to investigate HCl uptake on both amorphous and crystalline ices between 120 and 180 K. They considered ultrathin (10–100 layer thick) films of ice deposited on the W(100) surface[11,12] and on Pt(111) surface,[12,13] and they found that, within stoichiometric conditions, hexahydrate was present as an amorphous solid at 120 K. By increasing T ($T = 165$ K), amorphous hexahydrate was crystallized. If the H_2O to HCl ratio was less than 1:6, two coexisting phases were detected, formed by nearly pure ice and nearly pure $HCl–6H_2O$. George and co-workers[14] studied the HCl adsorption on ice at temperatures ranging from 140 to 186 K, using laser-induced thermal desorption. The ice film was deposited on Al_2O_3 substrate. At T below 148 K, the HCl and H_2O signals indicated rapid formation of an $HCl : 3\,H_2O$ trihydrate film, while the $HCl : H_2O$ ratio changed continuously between 148 and 175 K, with no observable stable $HCl : 6\,H_2O$ hexahydrate. Between 180 and 186 K, HCl uptake on ice increased by a factor of 50, an effect which was assigned to a roughness increase of the film surface.

Rieley *et al.*[15] measured that the probability of reversible uptake of HCl at the ice surface was nearly unity at T ranging between 80 and 120 K, while under stratospheric conditions, measurements by Leu,[16] and Hanson and Ravishankara[17] reasonably agreed around a value of 0.3. It was found that water ice at stratospheric temperatures could take up a large fraction of a monolayer and that adsorbed HCl was generally dissociated to ions, formed hydrates and was highly reactive. HCl mobility measurements indicated that the value of the bulk diffusion coefficient of HCl was very sensitive to the ice characteristics. This value was estimated around 10^{-12} $cm^2\,2\,s^{-1}$ at 158 K,[18] equal to 2×10^{-13} $cm^2\,s^{-1}$ at $T = 188$ K (Ref. 19) and less than 10^{-13} $cm^2\,s^{-1}$ for $T = 253$ K,[19] while other experiments[20] led to values ranging between 10^{-12} and 10^{-11} cm^2 s when T grew from 238 to 265 K. By contrast, no

[a]Also associated with the Universities of Aix-Marseille II and III.
[b]Fax: (33) 3 81 66 64 75. Electronic mail: claude.girardet@univ-fcomte.fr

conclusive HCl mobility measurement at the ice surface and interface could be reached.

Using a combination of laser-induced thermal desorption probing and isothermal desorption depth profiling, the diffusion kinetics of HDO on ultrathin (25–200 layer thick) HNO_3^- and HCl^- dosed crystalline D_2O ice multilayer grown epitaxially on Ru(001) support was investigated by George and co-workers[21] in the temperature range of 146–173 K. The HDO diffusion rate was shown to be 30–70 times slower in the presence of HNO_3 than into pure D_2O ice, while it was 10–20 times faster in the presence of HCl. These results that quantified the influence HNO_3 and HCl doses corresponding to initial coverages of 0.5–5 layers on the desorption kinetics of D_2O (Ref. 22) and the diffusion kinetics[21] were then used to determine the H_2O surface residence times extrapolated to stratospheric temperatures ranging between 180–210 K. These times were shown to be much longer than on pure ice in the presence of HNO_3 and much shorter in the presence of HCl. Unfortunately, no detectable surface diffusion kinetics for H_2O could be measured with or without acidic impurities, and only an upper limit for the diffusion coefficient less than 10^{-9} $cm^2\,s^{-1}$ was obtained at 140 K.

However and despite this wide experimental attention, it is not perfectly known how HCl is incorporated into the ice lattice and how the ice lattice responds to the presence of HCl on structural and dynamic points of view. Relevant questions are (i) whether the reaction mechanisms at the ice surface are ionic or molecular and (ii) whether the formation of a quasiliquid layer (QLL) is required or not to explain the large HCl uptake by ice under stratospheric condition, that is around 190–200 K. The existence of a QLL at the surface of ice in presence of HCl has been proposed by Molina[3] and Abbatt *et al.*[7] to explain the solvation of HCl and the observed large HCl uptake by ice crystals. However, several models supported by molecular dynamic simulations[23–25] have suggested that a QLL was not required to induce HCl ionization at 190 K.

In a previous experimental work based on neutron diffraction[26] and quasielastic neutron scattering[27] on a bare ice film adsorbed on a MgO(100) crystalline substrate, we have shown[27] that the ice film presented a high degree of order at 190 K, whereas surface disorder and melting occurred at 250 K$<T<$265 K. It was found that, at 265 K, the translational mobility of the surface water molecules was close to that of bulk normal water determined at temperature slightly above the melting point. The choice of considering a thin supported ice film instead of bulk ice crystal was dictated by the possibility that it offered to study experimentally a system whose size was comparable to the MD simulation box, making the comparison between experiments and theory more applicable. Especially, the simulations carried out simultaneously showed[27] that the effect of the MgO substrate changed only slightly the ice film behavior close to the ice/vapor surface as compared to the same ice film deposited on a bulk ice crystal.

In the present paper, we will focus our attention on the effect of HCl adsorption on a similar ice film deposited on the same substrate. The amount of HCl deposited onto the ice surface will be in the submonolayer range owing to possible application to atmospheric chemistry. We will compare the structural and dynamic modifications of the ice film under HCl adsorption with respect to pure ice in a large domain of temperature including that of the stratosphere. Our aim is to determine the physical state of the ice surface in the presence of HCl at submonolayer coverage and at temperatures relevant to PSCs, and therefore, to contribute to the debate on its possible role with respect to HCl adsorption, solvation and incorporation into ice crystals. In a companion paper (paper II),[28] we will continue the study by presenting MD simulations and a detailed description of the effects of HCl adsorption on ice. The quasielastic and neutron diffraction experiments are described in Sec. II. The results are presented separately in Sec. III. They are then discussed together and compared to simulation data.

II. EXPERIMENTS

A. Incoherent quasielastic neutron-scattering (QENS)

1. Experimental setup and sample preparation

Experiments have been performed at the Laboratoire Leon Brillouin (LLB) at Saclay (France) on the time of flight (TOF) spectrometer G6.2 (Mibemol). The wavelength has been set to 8 Å ($E_0=1.28$ meV) allowing a scattering vector range Q from 0.35 $Å^{-1}$ to 1.46 $Å^{-1}$. The energy resolution of the spectrometer is $\Delta E=39.4$ μeV. There is no ice nor MgO Bragg reflection within the experimental Q-range.

The MgO substrate that is obtained in our laboratory is a powder made of small cubes featuring very uniform (001) facets, as shown in many adsorption experiments.[29,30] The neutron cell is a stainless steal cylinder with a diameter of 2 cm and a height of 8 cm, that has been loaded with about 5 g of MgO powder. After calibration of the powder using methane adsorption isotherm at 77 K,[31] we can derive the value of the total adsorbing area of the powder equal to 47 $\pm$ 2 m^2.

The normal H_2O from Fluka, contains less than 3 $\times 10^{-6}$% of organic impurities, and it is further purified by many cycles of condensation at $T\cong 170$ K, pumping, evaporation, condensation. Hydrogen chloride used in our experiments is an HCl gas of ''electronic'' quality, 99.9% pure, coming from the Air Liquide company.

An equivalent five bilayers of hexagonal ice (BL) thick film is formed by using classical volumetry as explained in Ref. 31. A calibrated volumetric system allows us to introduce the desired amount of water into the neutron cell. The water introduction has been done at a MgO temperature of 250 K. Once the desired amount of gas is introduced, we slowly cool down the system at 190 K, the temperature at which the hydrogen chloride is adsorbed. The HCl coverage unit ($\Theta_{HCl}=1$) corresponds to one HCl molecule adsorbed per Mg surface site.

We have studied three HCl coverages, namely 0.3, 0.6, and 1.0 ML, at three different temperatures: 190, 220, and 250 K. All the spectra are obtained by subtracting the background signal due to the cell and MgO support. The counting times were about 14 h for each spectrum. The cryostat used is a so-called ''Orange cryostat'' of LLB working with liquid

helium and allowing to cool down the neutron cell from ambient temperature to 4 K. The temperature regulation system allows a temperature stability better than 5×10^{-2} K.

2. Description of the QENS models and fitting procedure

When a monochromatic incident neutron beam is scattered quasielastically by molecules containing hydrogen atoms, it measures the dominant incoherent scattering from them. The spectra are thus dominated by the Fourier transform of the self-correlation function of the H atoms. In liquid H_2O, the scattering law $S_{\text{incoh}}(Q,\omega)$ is generally written, in the quasielastic region, as the convolution of two factors: $S_t(Q,\omega)$ and $S_r(Q,\omega)$,[32] due to the translational and low-frequency rotational motions of the water molecules, respectively. The proton delocalization due to vibrations is taken into account via the Debye–Waller factor. In this model, the translational and rotational motions are decoupled, an assumption that is questionable in water, but has to be made to obtain a numerically tractable analytical model.[33] The translational and rotational components of the scattering law $S_{\text{incoh}}(Q,\omega)$ give rise to a broadening of the experimental elastic peak.

To reproduce the broadening due to the translational motions we have chosen a Brownian molecular motion model,

$$S_t(Q,\omega)=\frac{1}{\pi}\frac{D_tQ^2}{\omega^2+(D_tQ^2)^2}, \tag{1}$$

where Q is the scattering vector, $\hbar\omega=\Delta E$ is the energy gain or loss of the neutron, and D_t is the translational diffusion coefficient. In the case of anisotropic atomic displacements, we define the parallel $D_t^{\parallel}$ and normal $D_t^{\perp}$ components of this diffusion coefficient. Note that for a 2D diffusion, $D_t^{\parallel}=0$ and $D_t^{\perp}\neq0$, i.e., the atomic displacements are confined in a plane.[34] Integration of Eq. (1) over the isotropic distribution of crystallite orientations is required to calculate the powder average.

For the rotational component, an isotropic rotational diffusion model is chosen, in which the water molecules undergo free rotations limited by random collisions with nearest-neighbor molecules. The corresponding scattering law is the superimposition of a δ-function centered at $\omega=0$ and a sum of Lorentzian curves,

$$S_r(Q,\omega)=j_0^2(Q\rho)\,\delta(\omega)+\frac{1}{\pi}\sum_{l=1}^{\infty}(2l+1)j_l^2(Q\rho)\times\frac{l(l+1)D_r}{[l(l+1)D_r]^2+\omega^2}, \tag{2}$$

where $j_l^2(Q\rho)$ are the spherical Bessel functions, $\rho=0.98$ Å (the O–H distance) is a radius of gyration for the water molecule rotation,[35] and D_r is the rotational-diffusion coefficient.

Finally, the theoretical scattering function $S_{\text{incoh}}(Q,\omega)$ must be folded with the triangular-shaped QENS instrumental resolution, before being fitted to the measured spectra. We measure first the translational-diffusion coefficient D_t at small scattering vector values such as $D_t^{\perp}Q^2\ll D_r$. In these conditions, the broadening of the elastic peak comes essentially from the translational motion since the quasielastic broadening due to rotational motions vanishes at small Q values. It can be shown that the broadening obeys a D_tQ^2 law.[32] Next, the rotational-diffusion coefficient D_r is measured for higher scattering vector values. The theoretical scattering function is compared to the measured spectra. In order to find the best fit within all the experimental Q-range, we have varied three significant parameters: D_t, D_r, and the proportion of liquid phase in the film. The mean-square displacement $\langle u^2\rangle$ in the Debye–Waller factor is taken equal to 0.10 Å^2 under our experimental conditions. This value of $\langle u^2\rangle$ is somewhat intermediate between that of supercooled water[32] and that of ice films on Pt(111).[36]

B. Neutron-diffraction experiments

The experiment was performed on the G6.1 two-axis powder spectrometer at the Laboratoire Léon Brillouin (LLB) ($\lambda=4.738$ Å, $\Delta Q/Q=10^{-2}$). The MgO sample was prepared according to the method described in the previous Sec. II A. The adsorbing surface of the MgO powder sample has been calibrated from a methane volumetric adsorption isotherm measured at 77 K. We have found that our MgO powder sample corresponded to a total area of about 43 ± 2 m^2. Water introduction into the cell was performed at $T=250$ K. Nevertheless, to increase the diffracted signal and to reduce background from incoherent scattering by H atoms, we have used heavy water (D_2O). Indeed, deuterium has a larger coherent cross section than hydrogen. The heavy water used comes from Merck Company and it has a deuteration degree more than 99.95%. The water is further purified like in the QENS experiments. The HCl gas is the same as that used in the QENS experiments.

Once the desired amount of gas was introduced, we slowly cooled down the system at 190 K to introduce the same quantities of HCl gas as in the QENS study. Hence, we condensed 0.3, 0.6, and 1 ML of HCl at 190 K and the study was performed at three different temperatures: 190, 220, and 250 K. The counting times were about 12 h for each spectrum. The diffraction spectra are obtained by the difference between those of the substrate plus the adsorbate and those of the bare substrate plus the cell. The experimental diffraction peaks are adjusted by Gaussian functions. A least squares fit method is used to determine the positions, intensities and widths of the measured reflections. The Scherrer formula allows us to correlate these widths with the crystallite size.[37]

C. Results

1. Neutron diffraction

We have studied the structural effect of the HCl adsorption on the 5 BL thick ice film. Figure 1 represents the evolution of the thin ice film diffractogram vs the HCl coverage at $T=250$ K. We can see an important decrease of the Ih (100) peak intensity when the HCl coverage increases. At $\Theta_{\text{HCl}}=1$ ML the (100) peak disappears completely, while a bump appears at the same position, i.e., at $Q=1.61$ Å^{-1}. The other broad bump visible at all Θ_{HCl} values and situated at

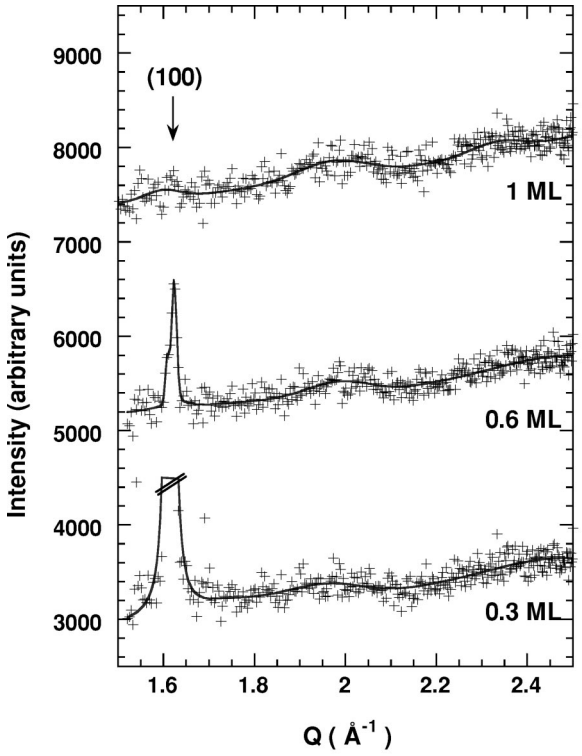

FIG. 1. Evolution of the neutron diffractograms of the 5 BL ice film vs the HCl coverage at $T=250$ K. Experimental spectra are represented by crosses and the solid lines are the best fits. The position of the (100) peak is shown by an arrow at $Q=1.61$ Å^{-1}.

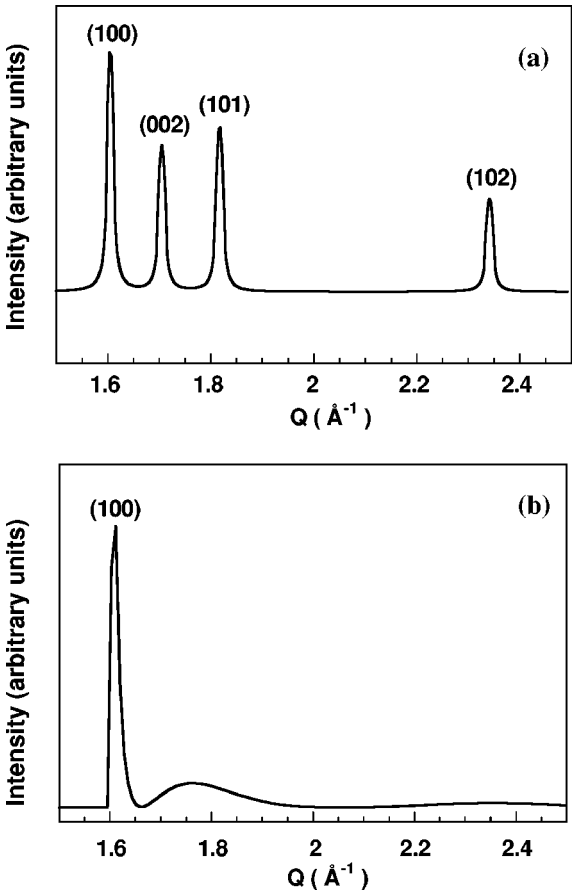

FIG. 2. Calculated powder spectra corresponding to (a) ice Ih (hexagonal lattice, $a=b=4.52$ Å, $c=7.37$ Å); (b) a 2 BL thick ice Ih film.

$Q\approx 1.99$ Å^{-1} could be attributed to the O–Cl distance equal to 3.14 Å.[38] However, our measurements cannot give any information about the ionic or atomic nature of Cl.

We have noticed that the ice Ih diffractogram at $T=250$ K (Fig. 1) differs from a typical ice Ih powder spectrum [Fig. 2(a)]. The peaks (002), (101), and (102), normally situated at $Q=1.71$ Å^{-1}, $Q=1.82$ Å^{-1}, and $Q=2.35$ Å^{-1}, respectively, are extinguished in our spectra. One possibility is that the innermost part of the solid ice Ih film would be very thin at $T=250$ K (less than or equal to two bilayers) while the other part of the film becomes liquid or amorphous. This hypothesis is supported by the shape of the calculated powder spectrum in Fig. 2(b) corresponding to a 2 BL hexagonal ice film (calculated with a coherence length $L=500$ Å). This spectrum exhibits a very intense (100) peak whereas, the others reflections are quasiextinguished. In particular, the (002) peak cannot be observed because it is too broad due to the lack of long range order in the direction perpendicular to the basal plane. The large bump situated at $Q\approx 1.75$ Å^{-1} represents the (101) peak not visible experimentally within the signal/noise ratio available in our neutron measurements. Furthermore, the presence of the outermost liquid phase is evidenced by our QENS experiments performed under the same conditions (see Sec. III B).

In Fig. 3, the evolution of the ice film diffractograms is shown vs the temperature for an HCl coverage of 1 ML. At $T=190$ K, the structure of the film corresponds almost exactly to the hexagonal ice structure, with the occurrence of the peaks (100), (002), (101), and (102). The coherence length found from the Scherrer formula is $L\approx 500$ Å. When the temperature rises to 220 K, new diffraction peaks appear at larger Q values, which correspond to the hydrogen chloride dihydrate phase[39] while the peaks assigned to ice decrease substantially. At higher T ($T=250$ K), all reflections disappear and are replaced by three bumps. The film becomes completely amorphous and/or liquid.

2. Quasielastic neutron scattering

Using quasielastic neutron scattering, we have measured spectra for different temperatures and HCl coverages (namely of 0.3, 0.6, and 1 ML). At these coverages and $T=190$ and 220 K, there is no measurable broadening of the peaks in the whole Q-range, indicating no translational mobility in the 5 BL ice film. Nevertheless we cannot rule out a translational motion leading to a quasielastic broadening smaller than the instrumental resolution ($D_t \leqslant 10^{-6}$ cm^2 s^{-1}).

In fact, a translational diffusion mobility becomes measurable at $T=250$ K. Figure 4 shows the evolution of the QENS signal as a function of the scattering vector at $T=250$ K and Fig. 5 displays its temperature behavior at a constant value of $Q=1.110$ Å^{-1}. The broadening of the elastic peak corresponds to a translational diffusion coefficient D_t of 0.8 (± 0.2)$\times 10^{-5}$ cm^2 s^{-1}. The estimated proportion of liquid in the film is about 30% for an HCl coverage of 0.3 ML, 45% at 0.6 ML and smaller than 9% at 1 ML. The rotational diffusion coefficient is equal to $D_r=1.8$ (± 0.3) $\times 10^{10} s^{-1}$ at $\Theta_{\mathrm{HCl}}=0.3$ and 0.6 ML, and its value decreases

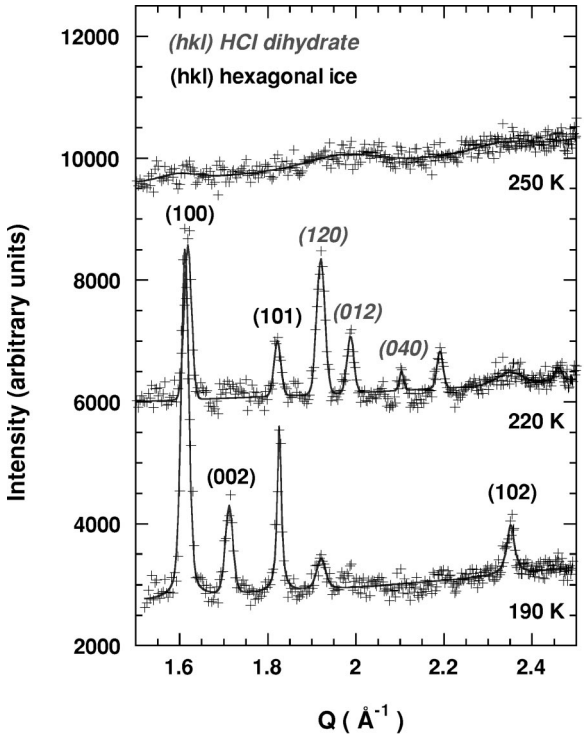

FIG. 3. Evolution of the neutron diffractograms of the 5 BL ice film with an HCl coverage of $\Theta_{HCl}=1$ ML vs temperature. Experimental spectra are represented by crosses and the solid lines are the best fits. Peak (hkl) written in italic correspond to the dihydrate phase.

to 7.0 $(\pm 1.0)\times 10^9$ s^{-1} at $\Theta_{HCl}=1$ ML. These values of the translational and rotational diffusion coefficients are of the same order of magnitude than those measured in Ref. 32 for supercooled water at the same temperature (see Table I).

D. Discussion

The neutron-diffraction experiments conducted at $T=190$ K show clearly that, whatever the HCl coverage is, the structure of the ice film corresponds to ice Ih. This structure appears to be unaffected by HCl adsorption, suggesting that HCl is mainly located at the surface of the ice film and does not penetrate the film. This experimental result is in very good agreement with the MD calculations presented in the companion paper.[28] Simulations at 190 K show that 75% of the HCl molecules are trapped at the surface of the ice film, while the remaining 25% lie inside the outermost bilayer.

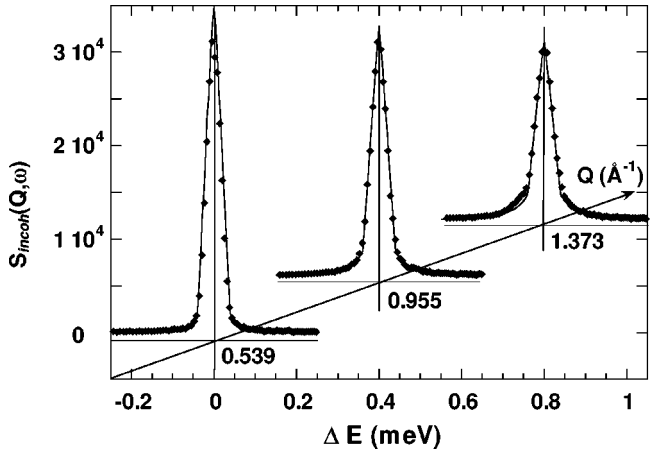

FIG. 4. Evolution of the QENS spectra measured at $T=250$ K vs the scattering vector, for an HCl coverage $\Theta_{HCl}=0.6$ ML. Experimental spectra are represented by full diamond symbols and the solid lines are the best fits.

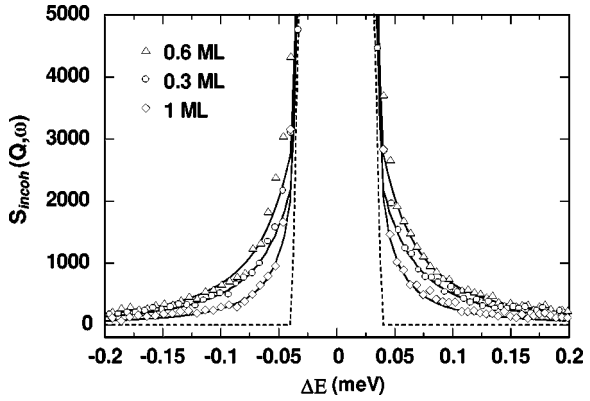

FIG. 5. Evolution of the QENS spectra at $Q=1.110$ $Å^{-1}$ vs HCl coverage. Experimental spectra are represented by empty symbols and the solid lines are the best fits for each HCl coverage. The dashed line represents the experimental resolution.

When T rises, no hydrate is observed at all temperatures studied for coverages 0.3 and 0.6 HCl monolayers. At $T=250$ K, only the (100) peak of the ice hexagonal structure remains. This result indicates that the ice film is thin, likely one or two BL thick, showing that the hexagonal structure of the ice film is destroyed except for the deepest layers close to the ionic support. For an HCl coverage of 1 ML, the hydrogen chloride dihydrate coexists with the hexagonal ice at $T=220$ K. However, the absence of the (002) peak characteristic of bulk ice still suggests that the ice Ih film is very thin. We interpret this feature by the fact that, only one part of the film corresponds to the hydrate phase, while the other part corresponds to the hexagonal phase. As suggested by the MD calculations presented in the companion paper,[28] at $T\geqslant 210$ K, HCl easily diffuses inside the ice film and destroys the ice Ih structure, except close to the MgO support where some order persists.

The existence of the dihydrate phase needs to be confronted to the bulk water/HCl phase diagram[40–43] shown in Fig. 6. We have reported in this figure our HCl concentrations if we suppose that HCl has mixed uniformly inside the water film. We see that, at $T=220$ K and 1 ML coverage, we are in principle very close to the trihydrate domain, whereas

TABLE I. Values of the translational and rotational diffusion coefficients D_t and D_r vs the HCl coverage Θ_{HCl} on the ice film at $T=250$ K. The corresponding liquid proportions are given. The values of D_t and D_r for pure supercooled liquid water at the same temperature are also given for comparison.

Θ_{HCl} (ML)	D_t (10^{-5} cm^2 s^{-1})	D_r (10^{11} s^{-1})	Liquid proportion
0.3	0.80 ($\pm$0.2)	0.18 ($\pm$0.03)	30%
0.6	0.80 ($\pm$0.2)	0.18 ($\pm$0.03)	45%
1	0.80 ($\pm$0.2)	0.07 ($\pm$0.01)	$\leqslant$9%
Water at 250 K[a]	0.4	0.8	⋯

[a]Reference 32.

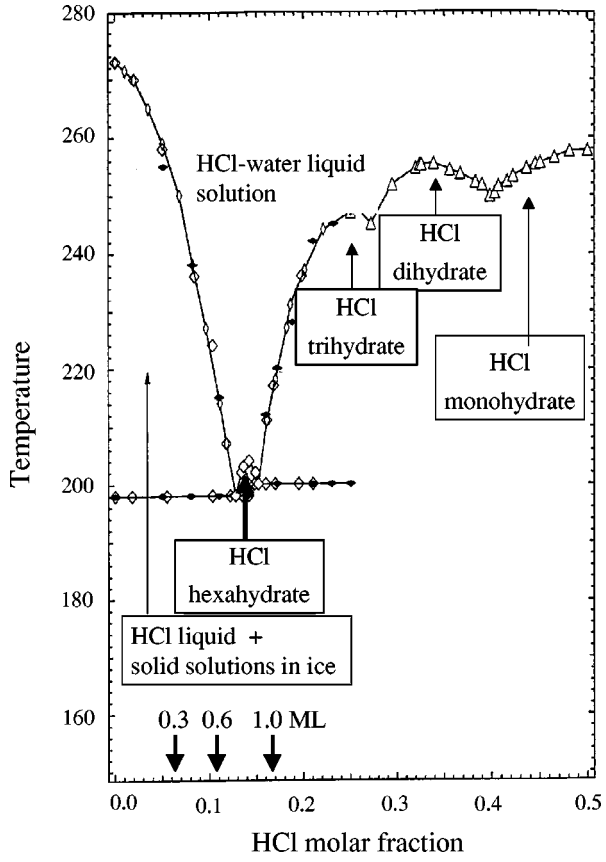

FIG. 6. Equilibrium phase diagram for the HCl/water system as a function of temperature and HCl molar fraction (see Refs. 39–42). The present experimental molar fractions are shown by arrows. The symbols, empty diamond, empty triangle, empty lozenge, and full diamond, correspond to experimental data issued from Refs. 41, 42, 43, and 40, respectively.

we do not observe the trihydrate but the dihydrate, instead. This discrepancy cannot be explained on the basis of the bulk phase diagram. However we cannot rule out special effects of the interfaces in such a thin ice film, especially of the MgO support which may influence the behavior of the ice/HCl film, modifying the HCl concentration close to the interfaces. These effects are corroborated by the simulations. Indeed, almost 45% of the HCl molecules are trapped at the gas/ice and MgO/ice interfaces while the other half is quasihomogeneously distributed in the bulk film. Hence, the HCl concentration is larger in the interfacial regions.

At $T=250$ K and $\Theta_{HCl}=1$ ML, the diffractogram does not display any narrow diffraction peaks. The ice/HCl film probably becomes an amorphous solid phase, which coexists with a small amount of liquid phase. As indicated by the QENS analysis, the liquid proportion is weak under these conditions ($\leqslant 9\%$). An amorphous solid phase has never been reported, as shown in the bulk water/HCl phase diagram in Fig. 6. One possible explanation is that upon warming, the HCl concentration becomes more homogeneous, moving our experimental point toward lower concentrations. If such is the case, and according to the bulk phase diagram shown in Fig. 6, our water/HCl film would have reached the region of the liquids. That would mean that the diffusion coefficient for this liquid at $T=250$ K is lower than 1×10^{-6} $cm^2 s^{-1}$, the smallest value of D_t we can measure on the Mibemol QENS spectrometer. The 9% mobile phase found in our analysis could well be a thin liquid layer close to the water/vapor interface.

For $\Theta_{HCl}=0.3$ and 0.6 ML, the liquid proportion found at $T=250$ K corresponds to a film thickness of about one or two layers (namely, 30% and 45% of the ice film thickness). Since the (100) ice Ih peak is still visible, we believe that only one part of the film is liquidlike with a mobility that is close to the value of liquid water. MD calculations performed in the companion paper show that this mobility concerns preferentially the outermost layers, i.e., the occurrence of the surface premelting.

In a previous paper,[27] we have studied the dynamical behavior of a 5 BL pure ice film, and have shown that a quasiliquid water layer of monolayer thickness exists at $T=265$ K. In the present results, we show that this quasiliquid layer appears at lower temperature ($T=250$ K) and that its thickness depends on the HCl coverage. This feature can thus be assigned to the HCl/water interactions responsible for an increasing disorder, via the entropic contributions. Our experiments indicate that, at the lowest stratospheric temperature ($T\approx190$ K), there is no quasiliquid layer having translational mobility of a normal liquid ($D_t\approx10^{-5}$ $cm^2 s^{-1}$) at the ice surface. The existence of a QLL was suggested by Molina *et al.*[6] to explain the solvatation and the diffusion of HCl in the ice crystals of the PSC's clouds. If a QLL would exist at these temperatures, its translational diffusion coefficient should be less than 10^{-6} $cm^2 s^{-1}$, i.e., the lowest detection limit we can reach in our QENS experiments. Hence, we can reasonably rule out the existence of a QLL at 190 K. This conclusion is in agreement with previous theoretical works by Kroes[44] and Gertner and Hynes.[23,24]

ACKNOWLEDGMENTS

The authors wish to thank R. Kahn and I. Mirebeau for accepting to be the local contacts on Mibemol and G61 spectrometers and for their help at LLB.

[1] S. Solomon, R. R. Garcia, F. S. Rowland, and D. J. Wuebbles, Nature (London) **321**, 755 (1986).
[2] S. Solomon, Nature (London) **347**, 347 (1990).
[3] M. J. Molina, in *Chemistry of the Atmosphere: Its Impact on Global Change*, edited by J. G. Calvert (Blackwell Scientific, Oxford, 1994), p. 27.
[4] R. P. Turco, O. B. Toon, and P. J. Hamill, J. Geophys. Res. **94**, 16493 (1989).
[5] J. Goodman, O. B. Toon, R. F. Pueschel, K. G. Snetsinger, and S. J. Verma, J. Geophys. Res. **94**, 16449 (1989).
[6] M. J. Molina, R. Zhang, P. J. Wooldridge, J. R. McMahon, J. E. Kim, H. Y. Chang, and K. D. Beyer, Science **261**, 1418 (1993).
[7] J. P. D. Abbatt and M. J. Molina, Geophys. Res. Lett. **19**, 461 (1992).
[8] J. P. D. Abbatt, K. D. Beyer, A. F. Fucaloro, J. R. McMahon, P. J. Wooldridge, R. Zhang, and M. J. Molina, J. Geophys. Res. **97**, 15819 (1992).
[9] P. A. Newman, J. F. Gleason, R. D. McPeters, and R. S. Stolarski, Geophys. Res. Lett. **24**, 2689 (1997).
[10] L. Delzeit, B. Rowland, and J. P. Devlin, J. Phys. Chem. **97**, 10312 (1993).
[11] J. D. Graham and J. T. Roberts, J. Phys. Chem. **98**, 5974 (1994).
[12] J. D. Graham and J. T. Roberts, Geophys. Res. Lett. **22**, 251 (1995).
[13] J. D. Graham and J. T. Roberts, Chemom. Intell. Lab. Syst. **37**, 139 (1997).
[14] K. L. Foster, M. A. Tolbert, and S. M. George, J. Phys. Chem. A **101**, 4979 (1997).
[15] H. Rieley, H. D. Aslin, and S. Haq, J. Chem. Soc., Faraday Trans. **91**, 2349 (1995).

[16] M. T. Leu, Geophys. Res. Lett. **15**, 17 (1988).
[17] D. R. Hanson and A. R. Ravishankara, J. Phys. Chem. **96**, 2682 (1992).
[18] L. T. Chu, M. T. Leu, and L. F. Keyser, J. Phys. Chem. **97**, 7779 (1993).
[19] B. G. Koehler, A. M. Midlebrook, and M. A. Tolbert, J. Geophys. Res. **97**, 8065 (1992).
[20] E. Thibert and D. Domine, J. Phys. Chem. B **101**, 3554 (1997).
[21] F. E. Livingston and S. M. George, J. Phys. Chem. **203**, 4366 (1999) and previous paper quoted therein on pure D_2O films.
[22] F. E. Livingston and S. M. George, J. Phys. Chem. A **102**, 102802 (1998).
[23] B. J. Gertner and J. T. Hynes, Science **271**, 1563 (1996).
[24] B. J. Gertner and J. T. Hynes, Faraday Discuss. **110**, 301 (1998).
[25] M. Svanberg, J. B. C. Petterson, and K. Bolton, J. Phys. Chem. A **104**, 5787 (2000).
[26] B. Demirdjian, J. Suzanne, D. Ferry, J. P. Coulomb, and L. Giordano, Surf. Sci. **462**, L581 (2000).
[27] C. Toubin, S. Picaud, P. N. M. Hoang, C. Girardet, B. Demirdjian, D. Perry, and J. Suzanne, J. Chem. Phys. **114**, 6371 (2001).
[28] C. Toubin, S. Picaud, P. N. M. Hoang, C. Girardet, B. Demirdjian, D. Ferry, and J. Suzanne, J. Chem. Phys. **116**, 5150 (2002), following paper.
[29] J. P. Coulomb and O. E. Vilches, J. Phys. (Paris) **45**, 1381 (1984).
[30] J. P. Coulomb, T. S. Sullivan, and O. E. Vilches, Phys. Rev. B **30**, 4753 (1985).
[31] J. P. Coulomb, K. Madih, B. Croset, and H. J. Lauter, Phys. Rev. Lett. **54**, 1536 (1985).
[32] S. H. Chen and J. Teixera, Adv. Chem. Phys. **64**, 20 (1986).
[33] M. Bée, *Quasielastic Neutron Scattering* (Adam Hilger, Bristol, 1988).
[34] A. J. Dianoux, F. Volino, and H. Hervet, Mol. Phys. **30**, 1101 (1970).
[35] J. Teixeira, M. C. Bellissent-Funel, S. H. Chen, and A. J. Dianoux, J. Phys. (Paris) **45**, C765 (1984).
[36] N. Materer, U. Starke, A. Barbieri, M. A. Van Hove, G. A. Somorjai, G. Kroes, and C. Minot, Surf. Sci. **381**, 190 (1997).
[37] L. Alexander and H. P. Klug, J. Appl. Phys. **21**, 137 (1950).
[38] N. Agmon, J. Phys. Chem. A **102**, 192 (1998).
[39] J. O. Lundgren and I. Olovsson, Acta Crystallogr. **23**, 966 (1967).
[40] K. Ji, thesis, Paris, France, 1994.
[41] S. U. Pickering, Ber. Bunsenges. Phys. Chem. **26**, 277 (1983).
[42] F. F. Rupert, J. Am. Chem. Soc. **31**, 851 (1909).
[43] G. Vuillard, C. R. Acad. Sci. Paris France **241**, 1308 (1955).
[44] G. J. Kroes, Comments At. Mol. Phys. **34**, 259 (1999).